

# Enhancement of nanocomposite materials properties based on $Y_2O_3$ filler and PVDF matrix

A. MATEI<sup>a,\*</sup>, V. ȚUCUREANU<sup>a,b</sup>, B. C. ȚÎNCU<sup>a,c</sup>, M. AVRAM<sup>a</sup>, C. ROMANIȚAN<sup>a,d</sup>, M. C. POPESCU<sup>a</sup>

<sup>a</sup>National Institute for Research and Development in Microtechnologies Bucharest, 126A, Erou Iancu Nicolae Street, 077190, Romania

<sup>b</sup>Transilvania University of Brasov, Department of Materials Science, 29, B-dul Eroilor, 500036, Romania

<sup>c</sup>University Politehnica of Bucharest, Faculty of Applied Chemistry and Materials Science, 1-7 Polizu, 011061 Bucharest, Romania

<sup>d</sup>Faculty of Physics, University of Bucharest, 405 Atomistilor Street, 077125, Magurele, Romania

The main purpose of the paper is to study the behavior of the  $Y_2O_3$  filler in the PVDF matrix and the use of materials synthesized as coating films. For the nanocomposites synthesis, in the incipient phase the polymer solution is obtained by dissolving the polymer in the corresponding solvent. Thus, composites were obtained by mixing the main components, followed by the ultrasonication step in order to obtain a well-dispersed solution and deposited on unconventional substrates. After deposition, the film was thermally treated at 80°C in order to remove the solvent and to densify the synthesized material. The impact of  $Y_2O_3$  filler on the morphological and structural properties of the matrix was investigated by FTIR, XRD, FE-SEM, EDX and contact angle. From the FTIR spectra analysis of the composite the presence of characteristic bands of the  $\alpha$  and  $\beta$  phase was observed. The XRD spectra indicate that the addition of the  $Y_2O_3$  did not modify the PVDF structure. SEM analysis shows that  $Y_2O_3$  particles are embedded in the matrix, and the interaction between the components has led to particle size growth through a slight agglomeration tendency. EDX spectra of the composite indicate the presence of the two components, the contact angle show the improvement of hydrophobic character of the nanocomposite film.

(Received January 7, 2019; accepted August 20, 2019)

**Keywords:**  $Y_2O_3$ , PVDF, Nanocomposites

## 1. Introduction

The benefits and properties of nanocomposite materials have generated an extensive research area, with increasing applicative potential in the aerospace industry and other related industries. The performance of the materials is in agreement with the selection of the main constituents of the composites, the compatibility and the interaction between the components, all of which determine the structure and properties of the nanocomposite material [1, 2].

Alternative approaches to improve the properties of composites are based on the advantages and characteristics of the main components, but also on the synergy between the individual phases, determining the synthesis of materials corresponding to the desired needs and meets the requirements specific to the application. Among the materials studied in the literature, the nanocomposites have experienced the most spectacular industrial development, generating by combining one or more components obtaining materials with improved properties and many other specific properties [3].

Generally, the nanocomposites refer to a multi-component system, which requires a detailed analysis of each of them for the selection of the main components: the matrix (majority constituent) and the filler (the minority constituent). The choice of the polymeric matrix is guided by their features, advantages and disadvantages, their physical, mechanical, thermal, optical and electrical

properties. Also, selecting the matrix is a complex matter, which must take into account the synergy between the constituent phases, the synthesis technology and the applicability field [4, 5].

One of the polymers studied is polyvinylidene fluoride (PVDF) extensively applied to scientific research and industrial processes for energy storage, water treatment, pollutants removal, separator for lithium ion battery, support for preparing composite membranes, mechanically-reinforced lightweight components, smart sensor devices and architectural coatings [4, 6-8].

Polyvinylidene fluoride (PVDF) is a semicrystalline polymer, which presents five different polymorphs,  $\alpha$  (form II, TGTG'),  $\beta$  (form I, TTTT),  $\gamma$  (form III, T<sub>3</sub>GT<sub>3</sub>G'),  $\delta$  and  $\epsilon$  depending on the chain conformation during the fabrication processes. Unique characteristics of PVDF such as high chemical resistance, outstanding thermal resistance, excellent, good degradation resistance against radiation, excellent piezoelectricity and pyroelectricity, high mechanical strength and inflammable, made it a base material for certain domains [9-13]. This polymer has been reinforced with various inorganic fillers with significant effect on the properties of the composite material in order to extend its applicability in a wide range of sectors (e.g. aerospace, automotive, civil engineering, healthcare and bio-medical, etc.). The choice of filler is based on the shape and properties of the particles, the dispersion degree, the compatibility criteria, the interfacial

effects, but also on the influence it exhibits to improve the performance of the material [14, 15, 40].

In the literature, there are researches involving the PVDF matrix with various fillers, such as ZnO, MgO, TiO<sub>2</sub>, Bi<sub>2</sub>O<sub>3</sub>, Al<sub>2</sub>O<sub>3</sub>, PZT, BaTiO<sub>3</sub>, etc. allowing to obtain nanocomposites used as water treatment membranes, removal of heavy metals, electronic devices, membranes for micro-bio-sensors, embedded capacitors/organic substrates, lithium-ion batteries, etc [9, 16-20, 41-43].

Another important criterion to be considered when choosing a filler is the synthetic method used to prevent the agglomeration phenomena and random distribution of particles. Often, in order to obtain PVDF matrix composites with filler used in the powder form, it is necessary an effective dispersion in the afferent matrix solvent (e.g. N, N-dimethylformamide, dimethyl sulfoxide, dimethylacetamide, triethylphosphate, 1,3 dioxolane, N,N'-dimethylpropyleneurea, methyl ethyl ketone, benzaldehyde, etc.), followed by mixing and sonication to produce a composite material with homogeneously distributed fillers [21-23].

The paper presents the behaviour (the degree of dispersion, incorporation and compatibility) of the Y<sub>2</sub>O<sub>3</sub> filler in the PVDF polymer matrix.

Yttria or yttrium oxide is an important inorganic compound with cubic symmetry, which has attracted special attention due to its outstanding physical and chemical properties, such as high melting point (2450 °C), high permittivity, high mechanical strength, high temperature stability, large optical band gap (~5.5eV), a relatively high dielectric constant (in the range 14-18), high thermal conductivity (0.13 WcmK<sup>-1</sup>) and an excellent electrical insulation (volume resistivity and dielectric breakdown strength). Also, the properties of this oxide depend on the crystalline structure and morphology in order to obtain performance material.

Based on its properties, Y<sub>2</sub>O<sub>3</sub> has a wide transparency varying from violet to infrared range; it possesses a good behaviour as coatings in various reactive environments, by preventing corrosion and resistance to aggressive chemical attack of the substrates. This material has numerous applications by using powerful microwave filters, advanced ceramics, luminescent devices, micro-electrochemical biosensors, etc. as additives in coatings at high temperature and in severe reactive environments [24-28].

The current challenges in this area of research are focused on the synthesis of Y<sub>2</sub>O<sub>3</sub>-PVDF composites, the dispersion of the Y<sub>2</sub>O<sub>3</sub> filler in the PVDF matrix using the same polar solvent (N-methyl-2-pyrrolidone, NMP) and the deposition of nanocomposite materials synthesized as coating films on unconventional substrate (in our experiments were used aluminum alloys).

The impact of Y<sub>2</sub>O<sub>3</sub> filler on the morphological and structural properties of the PDVF matrix was investigated by Fourier transform infrared spectroscopy (FTIR), X-ray diffraction (XRD), field emission scanning electron microscopy (FE-SEM), energy dispersive X-ray analysis (EDX) and contact angle (CA).

## 2. Experimental

### 2.1. Materials

Yttrium oxide powder was supplied by IMT-Bucharest (obtained by co-precipitation method). Poly(vinylidene fluoride) (PVDF, (C<sub>2</sub>H<sub>2</sub>F<sub>2</sub>)<sub>n</sub>-, powder with average M<sub>w</sub> ~ 180.000) and N-methyl-2-pyrrolidone (NMP, C<sub>5</sub>H<sub>9</sub>NO, M<sub>w</sub> = 99.13 g/mol) were acquired from Sigma-Aldrich and used as received.

### 2.2. Synthesis of Y<sub>2</sub>O<sub>3</sub>-PVDF nanocomposites materials

In the incipient phase, PVDF powder was dissolved in polar solvent of N-methyl-2-pyrrolidone (NMP) under continuously stirring at a constant temperature of 70°C until the formation of a homogeneous solution of 5% (w/v) concentration. The dissolution time varies depending on the molecular weight of the polymer, the solvent used and processing conditions [23, 29].

The secondary phase of the synthesis process consisted in dispersing the Y<sub>2</sub>O<sub>3</sub> filler into the afferent matrix solvent in order to minimize particle agglomeration, to ensure a good distribution and compatibility with the PVDF matrix. Finally, the two main components (PVDF matrix and Y<sub>2</sub>O<sub>3</sub> filler), in a 5:1 ratio, were contacted by continuous mechanical mixing at a constant temperature of 70 °C followed by sonication for 3 h at room temperature in order to obtain a well-dispersed solution.

The Y<sub>2</sub>O<sub>3</sub>- PVDF composites were deposited as films of varying thickness (between 5-10 μm) on unconventional substrates of aluminum alloys type. After deposition, the coated substrates were thermally treated at 80 °C to remove the solvent and densify the synthesized material.

The dispersion mode of the filler into the polymer matrix is largely influenced by the evaporation rate of the solvent, so that, by a slow evaporation a non-uniform distribution of the filler and pores formation can be achieved [30, 31].

These types of nanocomposite materials based on polymeric matrices used as coating films on unconventional substrates have found their applicability especially in the aerospace field. By using of nanocomposites in this field is aimed the development of some multifunctional protection systems, in order to ensure a good thermal, chemical and mechanical resistance, as well as stability and durability.

### 2.3. Characterization

Fourier Transform Infrared spectroscopy (FTIR) using a Bruker Tensor 27 spectrometer equipped with an ATR Platinum holder, in the wavenumber range of 4000 - 400 cm<sup>-1</sup> by averaging 64 scans with a resolution of 4 cm<sup>-1</sup> was used to investigate the bond configuration of the samples.

X-ray diffraction measurements of the samples were recorded using a rotating anode SmartLab diffraction system (Rigaku Corporation, Japan) equipped with a

CuK $\alpha$  radiation and a tube operated at 40 kV and current at 75 mA. Data were collected at a scan rate of 4 °/min.

SEM image was acquired using an FEI Nova NanoSEM 630, with ultra-high resolution at high and low voltage in high vacuum of 1.6 nm @1kV. To increase the SEM images quality, a gold layer of about 10 nm was vaporized onto samples surface.

Energy-dispersive X-ray spectroscopy (EDX, Smart Insight AMETEK) was used to identify the elemental compositions of the samples. The EDX equipment is attached to the Scanning Electron Microscope (SEM) allowing the collection of elemental information about the specimen of the composite.

Contact angles were measured by using Theta optical tensiometer (KSV Instruments) equipped with the CAM 101 camera and the 1394 firewire interface. Deionized water was chosen as the liquid in our experiments. The measurements were carried out in least three points and the average was reported.

All the samples (polymer and composite films) were analyzed after deposition on aluminum alloys substrates and followed by thermal treatment in order to obtain a cross-linked films.

### 3. Results

#### 3.1. FTIR analysis

The chemical structure and bond vibrations of the filler with polymer matrix in order to obtain  $Y_2O_3$ -PVDF composite materials were investigated through FTIR spectroscopy.

The FTIR spectra of the PVDF polymer matrix and  $Y_2O_3$ -PVDF composite are presented in Fig. 1. The range 450-1500  $cm^{-1}$  offers information about the conformation isomerism of the chain by identification of characteristic phases of PVDF.

The matrix presents the main absorbance bands at 1404, 1212, 1175, 985, 795, 744, 618, 471  $cm^{-1}$  corresponding to the  $\alpha$ -phase of PVDF. According to other researches, it is considered that the band located at 1404  $cm^{-1}$  can be attributed to the  $CH_2$  wagging vibration. The vibration bands at 1212 and 1175  $cm^{-1}$  can be assigned to the asymmetrical and symmetrical stretching of  $CF_2$ , respectively. The absorption bands at 985 and 795  $cm^{-1}$  can be assigned to  $CH_2$  twisting and  $CF_2$  rocking vibration. The peaks positioned at 744 and 618  $cm^{-1}$  can be assigned to  $CF_2$  bending and C-C-C skeletal vibration. The band at 471  $cm^{-1}$  can manifest bending and wagging vibration of  $CF_2$  groups [32, 33].

From the FTIR spectra analysis of the  $Y_2O_3$ -PVDF composite (Fig. 1b) the presence of intense bands at 977, 856, 795, 762, 615, 531  $cm^{-1}$  characteristic for the  $\alpha$ -phase was observed, but also the weak bands at 1278, 840, 765 and 508  $cm^{-1}$  which are typical vibration characteristics of the  $\beta$  crystalline phase of PVDF. The characteristic bands of  $\beta$  phase identified at 840  $cm^{-1}$  can be related to a mixed mode of  $CH_2$  rocking and  $CF_2$  asymmetric stretching vibration; the band at 795  $cm^{-1}$  can be assigned to  $CF_2$  bending and skeletal bending mode, 765  $cm^{-1}$  could be the  $CH_2$  rocking mode. Also, the band 508  $cm^{-1}$  could be attributed to  $CF_2$  bending vibration mode [34, 35].

The spectral analysis reveals a slight displacement of the characteristic peaks of the polymer as a result of the embedding of the filler nanoparticles thus suggesting to surround them with the polymer and to form a core-shell structure.

The results indicate that the addition of  $Y_2O_3$  filler to the polymer matrix can induce a phase transition from  $\alpha$ -phase to the  $\beta$ -crystalline phases, so in the composite material both phases coexisting in PVDF.

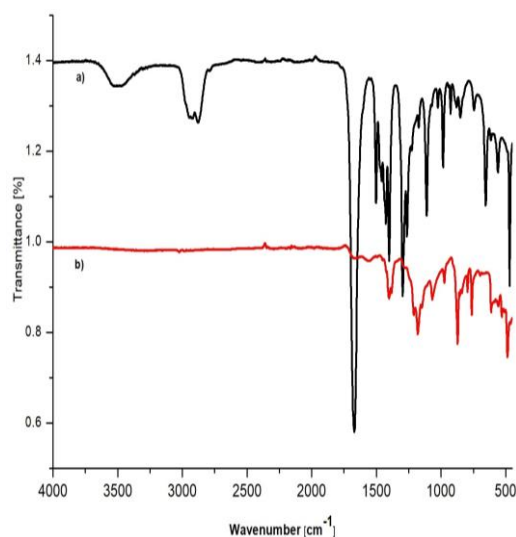


Fig. 1. FTIR spectra of a) PVDF and b)  $Y_2O_3$ -PVDF composite

#### 3.2. X-Ray diffraction analysis

The x-ray diffraction (XRD) analysis was used to determine the mean size of crystallite using Debye-Scherrer equation, the structure and degree of crystallization of the polymer matrix and  $Y_2O_3$ -PVDF composite materials.

The XRD diffraction spectra in the range  $2\theta = 5 - 90^\circ$  for the PVDF matrix and the  $Y_2O_3$ -PVDF composite are shown in Fig. 2.

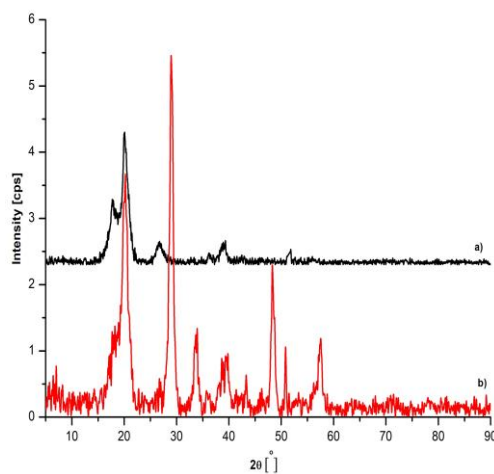


Fig. 2. XRD pattern of a) PVDF and b)  $Y_2O_3$ -PVDF composite

In the case of PVDF matrix (Fig. 2a), it is noted only the peaks characteristic of the  $\alpha$ -phase, occurring at  $2\theta = 17.95^\circ, 18.45^\circ, 20.04^\circ, 26.77^\circ$  and  $36.25^\circ$ , which are assigned to the lattice planes of (100), (020), (110), (021) and (200). The presence of the 5 predominate peaks of the  $\alpha$ -phase, indicates that this phase is formed during the crystallization process of neat PVDF.

The  $Y_2O_3$ -PVDF composite spectrum (Fig. 2b) reveals the semi-crystalline nature of the composites materials, identifying the peaks of the  $\alpha$  and  $\beta$  phases of the PVDF, but also the characteristic peaks of the  $Y_2O_3$  filler. By adding the filler in the matrix, it is observed the decreases of the peaks at  $17.95^\circ, 18.45^\circ$  characteristic of the  $\alpha$  phase, and the appearance as a shoulder of a peak at  $20.64^\circ$ , attributed to the (110)/(200) planes of the  $\beta$  phase in PVDF. It also highlights the presence of 3 peaks appeared at  $2\theta = 33.96^\circ, 38.76^\circ$  and  $43.33^\circ$  corresponding to the planes (130), (002) and (022) reflection of the monoclinic  $\alpha$ -phase, respectively.

All of these modifications demonstrate the reducing of  $\alpha$  phase and clearly reflects the formation of  $\beta$  phase in synthesized composite, which occurs due to both the presence of the filler in the matrix and the thermal treatment of the composite film at a temperature of  $80^\circ C$  [9, 36].

Generally,  $\alpha, \beta$  and  $\gamma$  phases of PVDF have an intense peak around  $20^\circ$ , thus it is difficult to distinguish from each other only by XRD analysis [37].

In the  $Y_2O_3$ -PVDF composite, the presence of diffraction peaks is observed of the  $Y_2O_3$  filler at  $2\theta = 29.04^\circ, 33.72^\circ, 39.27^\circ, 48.37^\circ$  and  $57.62^\circ$  corresponding to the planes (222), (400), (332), (440) and (622). The sharp peaks clearly show that the  $Y_2O_3$  filler retains its structure after the formation of the composite, but also it has an influence on the matrix's crystallinity.

Also, the XRD result shows that the PVDF matrix is completely  $\alpha$ -phase dominated, but the  $Y_2O_3$ -PVDF composite emphasize and the presence of  $\beta$  phase, which is in well agreement with the FTIR result.

The XRD spectra indicate a good interaction between the filler and the matrix, the two components coexisting in the  $Y_2O_3$ -PVDF composite material.

### 3.3. Morphological analysis

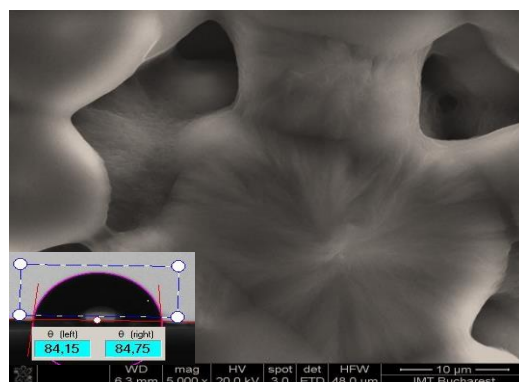
SEM was used to investigate the morphology, size, microstructure and the dispersion of in PVDF matrix in the presence of NMP solvent.

The surface of the PVDF film (Fig. 3a) indicates regions that contain pores and acicular crystallites emanating in the stretched direction from the centre. The result obtained indicate that the crystalline phase depends on the crystallization rate, so in this way the pores are clearly seen and interconnected with the acicular crystallites. The appearance of microstructure with high porosity degree and various sizes of pores may be due to evaporation of solvent and polymer crystallization at low temperature [38, 39].

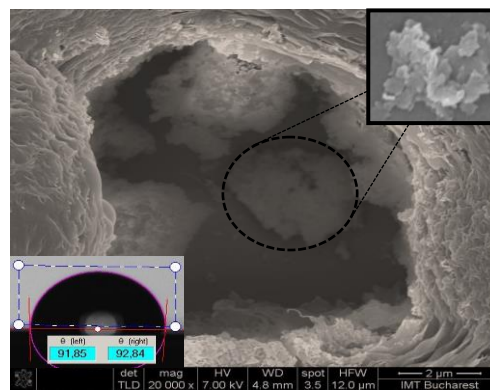
SEM microstructural analysis of the  $Y_2O_3$ -PVDF composites (Fig. 3b) shows that  $Y_2O_3$  particles are embedded in the polymer matrix, and the interaction between the two components (filler-matrix) has led to particle size growth through agglomeration tendency.

Due to the aggregation and non-uniform distribution of particles in the polymer matrix, it is difficult to calculate the average particle size.

The results obtained by measuring of contact angle indicate that the PVDF matrix present the hydrophilic character by low value of about  $84^\circ$ , and in the case of the  $Y_2O_3$ -PVDF composite the hydrophobic character was improved by increasing the contact angle around  $92^\circ$  confirming the positive influence of filler in polymer matrix.



(a)



(b)

Fig. 3. SEM images of a) PVDF and b)  $Y_2O_3$ -PVDF composite

### 3.4. EDX analysis

In order to determine the chemical composition of the  $Y_2O_3$ -PVDF composite sample, the energy dispersive X-ray (EDX) spectrum was recorded.

From EDX spectrum (Fig. 4) the purity of the obtained composite can be observed, the spectrum being defined only by peaks indicating the presence of the two components, such as: carbon (C) and fluorine (F) representing the presence of the PVDF structure; and, oxygen (O) and yttrium (Y) in the  $Y_2O_3$  filler.

The existence of Y and O in EDX spectrum indicates along with the specific peaks of matrix, come to confirm the coexistence of the two materials in different proportions, also confirmed by peak intensity.

The weight and atomic percentages (%) of the elements present in  $Y_2O_3$ -PVDF composite sample are shown in the related Table of the figure.

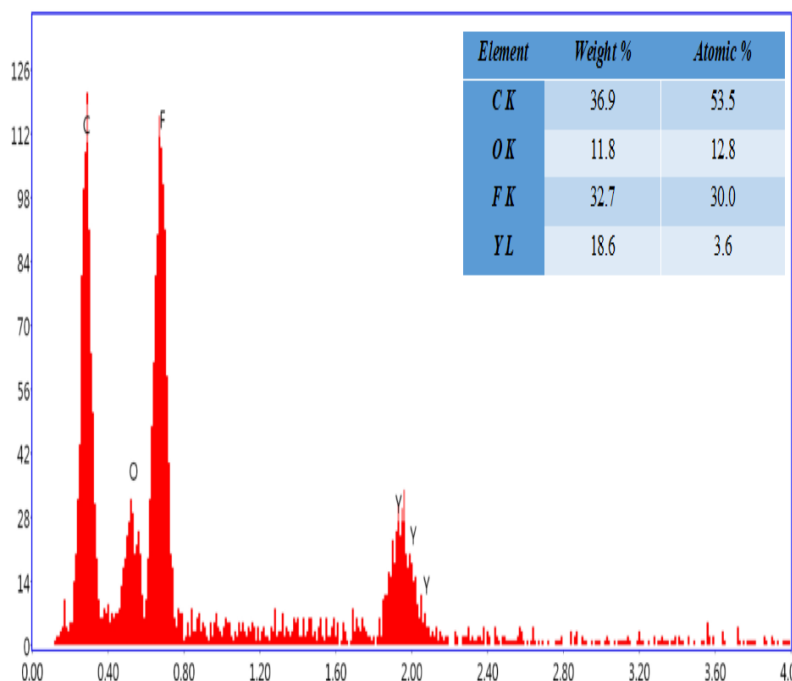


Fig. 4. EDX spectra of  $Y_2O_3$ -PVDF composite

Each characterisation technique approached for nanocomposite material was performed in ratio with the PVDF matrix, highlighting that by using  $Y_2O_3$  filler, the morpho-structural properties and hydrophobic character of the  $Y_2O_3$ -PVDF were improved.

#### 4. Conclusions

The  $Y_2O_3$ -PVDF composite was obtained by the ex-situ method by dispersing the  $Y_2O_3$  filler in the afferent matrix solvent, followed by contacting the two components by mixing and ultrasonography to disperse the aggregates and forming a dispersed solution. This composite was deposited as thin film on various unconventional substrates such as aluminum alloys.

The results of our research have shown that the degree of the filler dispersion in the polymer matrix was determined by the mixing process conditions and by the evaporation rate of the solvent. The impact of  $Y_2O_3$  filler on the morphological and structural properties of the PDVF matrix was investigated.

From the analysis of the FTIR spectra and XRD measurements, it is clearly highlighted the presence of  $\alpha$  phase and that the filler induces the formation of  $\beta$  phase in composite material.

SEM images confirm that the addition of filler particles in PVDF matrix, leads to the formation of agglomerate structure by inhomogeneous dispersion of the filler and the existence of voids causing the modification

in surface morphology. The purity of the synthesized composite is defined by the presence of elemental yttrium (Y) and the oxygen (O) of the filler nanoparticles and carbon (C) and fluorine (F) that represent the presence of PVDF structure.

The measurements made to determine the contact angle show a hydrophilic character of polymer matrix and the obtaining of hydrophobic composite films so necessary in aerospace field deposited on unconventional substrates.

All of these characteristics of the composites are important for their practical applications as coating systems for various substrates with applicability in specific fields.

#### Acknowledgements

This work was supported by a grant of the Ministry of National Education and Scientific Research, RDI Program for Space Technology and Advanced Research—STAR, project number 639/2017. Also, this work was supported by UEFISCDI in the Partnership Framework: PN-III-P1-1.2-PCCDI-2017-0214 (Project No. 3 PCCDI/2018).

#### References

- [1] V. T. Rathod, J. S. Kumar, A. Jain, 2017, Applied Nanoscience **7**, 519 (2017).
- [2] K. Muller, E. Bugnicourt, M. Latorre, M. Jorda, Y. E. Sanz, J. M. Lagaron, O. Miesbauer, A. Bianchin, S. Hankin, U. Bolz, G. Perez, M. Jesdinszki,

- M. Lindner, Z. Scheuerer, S. Castello, M. Schmid, *Nanomaterials* **7**(74), 1 (2017).
- [3] I. P. Jeon, J. B. Baek, *Materials* **3**, 3654 (2010).
- [4] C. C. Okpala, *International Journal of Advanced Engineering Technology* **5**(4), 12 (2014).
- [5] T. Hanemann, D. V. Szabo, *Materials* **3**, 3468 (2010).
- [6] G. D. Kang, Y. M. Cao, *Journal of Membrane Science* **463**, 145 (2014).
- [7] K. A. Wood, S. R. Gaboury, *Surface Coatings International Part B: Coatings Transactions* **89**, 231 (2006).
- [8] S. Moharana, M. K. Mishra, B. Behera, R. N. Mahaling, *International Journal of Engineering Technology, Management and Applied Sciences* **3**(4), 303 (2015).
- [9] A. Matei, V. Tucureanu, P. Vlazan, I. Cernica, M. Popescu, C. Romanițan, 2017, *AIP Conference Proceedings* **1916**(1), 030006-1-6 (2017).
- [10] X. Cai, T. Lei, D. Sun, L. Lin, *RSC Advances* **7**, 15382 (2017).
- [11] M. Haponska, A. Trojanowska, A. Nogalska, R. Jastrzab, T. Gumi, B. Tylkowski, *Polymers* **9**, 718 (2017).
- [12] Z. W. Ouyang, E. C. Chen, T. M. Wu, *Materials* **8**, 4553 (2015).
- [13] R. Gregorio, E. M. Ueno, *Journal of Materials Science* **34**, 4489 (1999).
- [14] M. S. Islam, R. Masoodi, H. Rostami, *Journal of Nanoscience* **2013**, 1 (2013).
- [15] S. Rathore, H. Mahhav, G. Jaiswar, *Materials Research Innovations* **23**(4), 183 (2017).
- [16] H. Razzaq, H. Nawaz, A. Siddiq, M. Siddiq, S. Qaisar, *Madridge Journal of Nanotechnology and Nanoscience* **1**(1), 37 (2016).
- [17] M. D. Rozana, A. N. Arshad, M. H. Wahid, M. N. Sarip, Rusop M., 2017, *International Journal of Research in Science* **3**(1), 8 (2017).
- [18] A. K. Chilvery, A. K. Batra, M. Thomas, *Physical Science International Journal* **4**(5), 734 (2014).
- [19] H. Wang, H. Li, L. Yu, Y. Jiang, K. Wang, *Journal of Applied Polymers* **130**(4), 2886 (2013).
- [20] I. Y. Abdullah, M. Yahaya, M. H. Jumali, H. M. Shanshool, *Optical and Quantum Electronics*, **149**(48), pp. 2 (2016).
- [21] M. Li, I. Katsouras, C. Piliago, G. Glasser, I. Lieberwirth, P. W. M. Bolm, D. M. de Leeuw, *Journal of Materials Chemistry C* **1**, 7695 (2013).
- [22] M. M. Tao, F. Liu, B. R. Ma, L. X. Xue, *Desalinization* **316**, 137 (2013).
- [23] C. Ribeiro, C. M. Costa, D. M. Correia, J. Nunes-Pereira, J. Oliveira, P. Martins, R. Gonçalves, V. F. Cardoso, S. Lanceros-Méndez, *Nature Protocol* **13**(4), 681 (2018).
- [24] M. Aghazadeh, M. Ghaemi, A. Golikand, T. Yousefi, E. Jangju, *ISRN Ceramics* **2011**, 1 (2011).
- [25] R. Srinivasan, R. Yogamalar, A. C. Bose, *Materials Research Bulletin* **45**, 1165 (2010).
- [26] Z. M. Larimi, A. Amirabadizadeh, A. Zelati, *International Conference on Chemistry and Chemical Process* **10**, 86 (2011).
- [27] K. J. Jeong, D. S. Bae, *Korean Journal of Materials Research* **22**(2), 78 (2012).
- [28] Z. M. Larimi, A. Amirabadizadeh, A. Zelati, *International Conferene on Chemisry and Chemical Process* **10**, 86 (2011).
- [29] M. Haponska, A. Trojanowska, A. Nogalska, R. Jastrzab, T. Gumi, B. Tylkowski, *Polymers* **9**, 718 (2017).
- [30] X. G. Tang, M. Hou, L. Ge, J. Zou, R. Truss, W. Yang, M. B. Yang, Z. H. Zhu, R. Y. Bao, *Journal of Applied Polymer Science* **125**, E592 (2012).
- [31] Y. C. Hu, W. L. Hsu, Y. Wang, C. T. Ho, P. Z. Chang, *Sensors* **14**, 6877 (2014).
- [32] A. M. Gaur, D. S. Rana, *Journal of Material Science: Materials in Electronics* **27**, 2293 (2016).
- [33] A. S. Elmezayyen, F. M. Reicha, I. M. El-Sherbiny, J. Zheng, C. Xu, *European Polymer Journal* **90**, 195 (2017).
- [34] R. Vinod, S. R. Achary, C. M. Tomas, V. Munoz-Sanjose, M. J. Bushiri, *Journal of Physics D: Applied Physics* **45**(42), 425103 (2012).
- [35] S. Lanceros-Méndez, J. F. Mano, A. M. Costa, V. H. Schmidt, *Journal of Macromolecular Science, Part B: Physics* **27**, 517 (2001).
- [36] K. Jurczuk, A. Galeski, M. Mackey, A. Hiltner, E. W. Baer, *Colloid and Polymer Science* **293**, 1289 (2015).
- [37] P. Fakhri, H. Mahmood, B. Jaleh, A. Pegoretti, *Synthetic Materials* **220**, 653 (2016).
- [38] A. Jain, J. S. Kumar, S. Srikanth, V. T. Rathod, D. R. Mahapatra, *Polymer Engineering and Science*, **53**(4), 707 (2013).
- [39] J. Nunes-Pereira, S. Ribeiro, C. Ribeiro, C. J. Gombek, F. M. Gama, A. C. Gomes, D. A. Patterson, S. Lanceros-Mendez, *Polymer Testing* **44**, 234 (2015).
- [40] A. Zia, S. Ahmed, N. A. Shah, *J. Optoelectron. Adv. M.* **20** (3-4), 180 (2018).
- [41] J. X. Gong, Y. T. Dai, H. Zhang, L. Y. Pu, W. Wang, *Optoelectron. Adv. Mater.* **12**(11-12), 744 (2018).
- [42] C. Miclea, F. C. Miclea, L. Amarande, C. T. Miclea, M. Cioanger, *J. Optoelectron. Adv. Materials* **20**(9-10), 558 (2018).
- [43] S. A. Ziahosseini, *Optoelectronics and Advanced Materials Rapid Communications* **13**(3-4), 273 (2019).

---

\*Corresponding author: alinaci.am@gmail.com